

Synergy Photodegradation of Basic Dyes by ZnO/Bi₂O₃ Nanocomposites under Visible Light Irradiation

Bhaviya Raj, Ramaraj; Umadevi, Mahalingam*⁺; Parimaladevi, Ramasamy

Department of Physics, Mother Teresa Women's University, Kodaikanal-624102, INDIA

ABSTRACT: Environmental problems caused by organic pollutants can be resolved by semiconductor photocatalysts. Using the strategies of doping hydrothermally, Zinc oxide/Bismuth oxide nanocomposites (ZnO/Bi₂O₃ NCs) comprising of different proportions of BiO for the applications of basic dyes and were tested for antibacterial activity. The average crystallite sizes of these, metal oxide nanocomposites were ranging from 12 nm to 29 nm. UV-Visible diffuse reflectance spectra were used to determine the optical energy bandgap (E_g) of about 2 to 2.82 eV of the NCs for different proportions of the metal oxides. Square-like morphology of ZnO NPs and ZnO/Bi₂O₃ NCs were observed in the Scanning Electron Microscopy (SEM). This morphological structure along with its high surface area attributes to the promotion of degrading organic pollutants in dyeing wastewater along with decolorization. The Photoluminescence (PL) emission intensity of ZnO/Bi₂O₃ NCs suggests a lower recombination rate of photogenerated charge carriers leading to enhanced photocatalytic activity. Visible light-driven photodegradation of MB, MG, and R6G by 0.5M ZnO: 0.5M Bi₂O₃ resulted in high rate constants of $8.5 \times 10^{-3}/\text{min}$, $6 \times 10^{-3}/\text{min}$, and $9 \times 10^{-3}/\text{min}$. The hybrid ZnO/Bi₂O₃ NC materials showed immense antibacterial activity against gram-positive bacterium *S. aureus* and the gram-negative bacterium *E. coli* with an inhibition zone of 6mm and 5mm respectively which was comparable to the standard, chloramphenicol. A desired predominant gram-positive bacterial inhibition unwraps a new way for enhanced antibacterial agents. The heterojunction at the interface between Bi₂O₃ and ZnO could efficiently reduce the recombination of photoinduced electron-hole pairs and thereby enhancing the photocatalytic and antibacterial activity of ZnO/Bi₂O₃ heterostructures. This study reveals that ZnO/Bi₂O₃ NCs as a promising candidate for the photocatalytic and antibacterial treatment of dye effluent.

KEYWORDS: ZnO/Bi₂O₃ nanocomposites; X-ray diffraction; energy bandgap; photoluminescence; photocatalytic activity; antibacterial activity.

INTRODUCTION

Water is basic and obligatory to all living beings. The emerging environmental contaminants in water have posed serious threats to living beings. Semiconductor

photocatalyst has great potential in resolving environmental problems caused by organic pollutants [1]. Dyeing industries are the most polluting industries worldwide [2].

* To whom correspondence should be addressed.

+ E-mail: ums10@yahoo.com

1021-9986/2021/4/1121-1131

11/\$/6.01

Ample treatment of wastewater, along with the ability to provide a sufficient supply of clean water, has become a major concern for many communities. Purification of water to degrade organic pollutants using photocatalysts by photocatalytic degradation is a useful technology. Multifunctional and eco-friendly Nanocomposites (NCs) have drawn tremendous attention in the field of nanomaterial science. Semiconductor photocatalysts provide a potential solution to many environmental pollution problems faced by mankind. Semiconductor photocatalysts generally absorb different color light depending on their bandgap energy and are used as photocatalysts because of their interesting electronic configurations, light absorption ability, charge carrier transport property, and excited-state lifetimes [3,4].

Among various synthesis methods of nanoparticles, hydrothermal remains to be the most convenient, cheapest, and pollution-free. Zinc oxide (ZnO) is a semiconductor with potential application in photocatalysis. The nano-sized ZnO particles with tremendous scientific and technological interest due to their attractive properties such as biosafety, high stability, wide direct bandgap (3.37 eV), and high exciton binding energy of 60 meV. ZnO has gained immense attention due to its unique catalytic, UV-filtering, antibacterial, anti-inflammatory, antifungal properties owing to its large surface area to volume ratio [5]. The performances of nanosized ZnO as photocatalysts and antibacterial agents can be influenced by doping metal ions into ZnO. Doping affects the dynamics of electron-hole pair recombination and interfacial charge transfer. Bi-based oxides have been found to be very active under visible light irradiation, which is attributed to the hybridized valence band by O 2p and Bi 6s so as to narrow the bandgap [6]. Bismuth oxide (Bi₂O₃), as a promising semiconductor and is an attractive material for the photooxidation of pollutants because of its direct bandgap of 2.8 eV [7], photoluminescence, high oxygen-ion conductivity, high refractive index, and dielectric permittivity [8].

Anxiety in living beings has been occurred due to the release of organic pollutants into the environment. Among the synthetic dyes, Azo dyes contain one or more azo bonds and are the most widely used synthetic dyes and are extensively used in the textile dyeing industry [9]. Dye wastewater from textile industries was contributing significantly to water pollution due to its aesthetically

improper color and toxicity to aquatic flora/fauna and also for human beings [10]. Moreover, dye-containing effluents are a major threat, as organic pollutants are released as wastewater in the ecosystem. The inappropriate disposal of dyes in wastewater constituents is an environmental problem causing damage to the ecosystem. Hence the removal of organic pollutants from wastewater by heterogeneous photocatalysis is an important method in environmental protection. Photocatalytic degradation for purifying wastewater has attracted much attention [11]. The highly reactive hydroxyl radicals (OH[•]) generated in the photocatalytic oxidation process thereby emerges as a promising wastewater treatment technology in the degradation of organic contaminants under irradiation. The photoactivated reactions are characterized with the aid of the unfastened radical mechanism initiated via the interplay of photons of a definite energy level, with the photocatalysis reaction ensuing in the degradation of diverse organic impurities. The higher the effective surface area, the higher will be the adsorption of target molecules leading to better photocatalytic activity. R. Saravanan et al., [12] studied the photocatalytic degradation of methylene blue and methyl orange under visible light irradiation in the presence of various percentages of composite catalyst synthesized by thermal decomposition method. V.L. Chandraboss et al., [13] have studied the effect of Bismuth doping on the ZnO nanocomposite material and study of its photocatalytic activity under UV light. Tongqin Chang et al., [14] demonstrated the synthesis of the ZnO/ Bi₂O₃ nanocomposites by two-step hydrothermal methods and its photodegradation of methylene blue and methyl orange. Weidong et al., [15] studied the photocatalytic properties of bismuth oxide films prepared through the sol-gel method. Nanoparticles that can limit or destroy without toxicity to the host, organisms are most important for healthier living [16]. Although there are some studies reported on the photocatalytic activity by ZnO/Bi₂O₃, treating basic dyes with different concentrations of Bi₂O₃ in ZnO under visible light and study of its antibacterial activity against human pathogenic bacteria *S. aureus* (gram-positive) and *E. coli* (gram-negative) has not been reported to the best of our knowledge. Hence the main objective of this work is to hydrothermally synthesize ZnO NPs, Bi₂O₃ NPs, and ZnO/Bi₂O₃ nanocomposites (NCs) and to evaluate them as efficient photocatalysts against basic dyes and antibacterial activity against *S. aureus* and *E. coli*.

EXPERIMENTAL SECTION

Materials

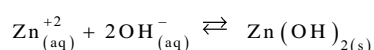
Zinc nitrate hexahydrate (Zn(NO₃)₂ · 6H₂O) (Merck), sodium hydroxide NaOH (Merck), and Bismuth nitrate pentahydrate (Bi(NO₃)₃ · 5H₂O) (Merck), distilled water, and ethanol were purchased and used without further purification.

Preparation of ZnO NPs, Bi₂O₃ NPs, and ZnO/Bi₂O₃ NCs

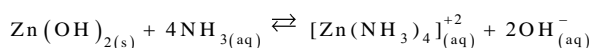
The synthesis procedure was done as in literature [17] with slight modifications. To prepare ZnO NPs hydrothermally, 1M solution of Zn(NO₃)₂ · 6H₂O in NaOH solution was magnetically stirred and heated in Teflon autoclave for 5h at 100°C in an oven. The resultant precipitate was filtered and washed several times with distilled water and ethanol to remove impurities and dried at 80°C.

To prepare Bi₂O₃ NPs hydrothermally, 1M solution of Bi(NO₃)₃ · 5H₂O in NaOH solution was magnetically stirred and heated in Teflon autoclave for 5h at 100°C in an oven. The resultant precipitate was filtered and washed several times with distilled water and ethanol in order to remove impurities and dry at 80°C.

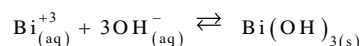
0.1 M, 0.3 M and 0.5 M Bi(NO₃)₃ · 5H₂O were added to 0.9 M, 0.7 M and 0.5 M of ZnO in NaOH solution respectively to prepare ZnO/Bi₂O₃ NCs (0.9M ZnO: 0.1M Bi₂O₃, 0.7M ZnO: 0.3M Bi₂O₃ and 0.5M ZnO: 0.5M Bi₂O₃ NCs). In this reaction Zn(NO₃)₂ · 6H₂O and Bi₂O₃ · 5H₂O reacts with NaOH, precipitates Zn²⁺_(aq) into zinc hydroxide Zn(OH)₂ along with the formation of ZnO NPs.



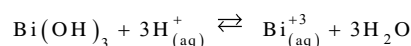
The Zn(OH)₂ can be distinguished from ZnO NPs by using excess ammonia as Zn(OH)₂ dissolves in excess ammonia.



NaOH with Bi(NO₃)₃ · 5H₂O, Bi³⁺ precipitates into Bi(OH)₃ along with Bi₂O₃ NPs. Bi(OH)₃ can be distinguished from Bi₂O₃ NPs by using acids.



Because Bi(OH)₃ does not dissolve in excess ammonia but dissolves in acids.



So by using ammonia and dilute acids, Zn(OH)₂ and Bi(OH)₃ can be distinguished with NPs. The autoclaved solution at 100°C in an oven for about 5h was filtered and washed with distilled water and ethanol to remove impurities and dried at 80°C.

Characterization techniques

The structural analysis was carried out by using a powder Burker advanced X-ray diffractometer with Cu-Kα radiation (λ=1.54 Å). The surface morphology and composition of the ZnO/Bi₂O₃ NCs were examined by Scanning Electron Microscope (SEM, FEI Quanta 200) equipped with the Energy Dispersive X-ray spectrometer (EDX, Oxford instruments-INCAx). The photoluminescence spectra were analyzed by a Jobin Yvon Fluorimeter. The absorbance spectra were measured using the Shimadzu (UV 1700) UV-Vis spectrophotometer.

Photocatalytic measurements

The photocatalytic activity of the ZnO NPs, Bi₂O₃ NPs, and ZnO/Bi₂O₃ NCs was evaluated by the photocatalytic degradation of organic pollutants in basic dyes such as Methyl blue (MB), Malachite green (MG), and Rhodamine 6G (R6G). In this experiment, 0.01 g of ZnO NPs, Bi₂O₃ NPs, and ZnO/Bi₂O₃ NCs were dispersed in 50 mL of basic dyes separately. The suspensions were irradiated using visible light at room temperature over a time period of 120 min and the absorbance changes were studied at 10 min intervals along with the degradation.

Antibacterial assay

The antimicrobial activities of ZnO NPs, Bi₂O₃ NPs, and ZnO/Bi₂O₃ NCs were evaluated against the Gram-positive pathogen *S. aureus* and Gram-negative *E. coli*, by the disc diffusion method. A different concentration of the extracts (100 µg/mL) was prepared by reconstituting with methanol. The test microorganisms were routed through the respective medium by spread plate method (10 µL (10 cells/mL)) with the 24h cultures of bacteria growth in a nutrient broth. After solidifying, the filter paper wells with extricates were infused on test organism-seeded plates. Chloramphenicol (10 µg) was used as the standard for the antibacterial test. The antibacterial assay plates were incubated at 37 °C for 24 h. The diameters of the inhibition zones were measured in millimeter (mm).

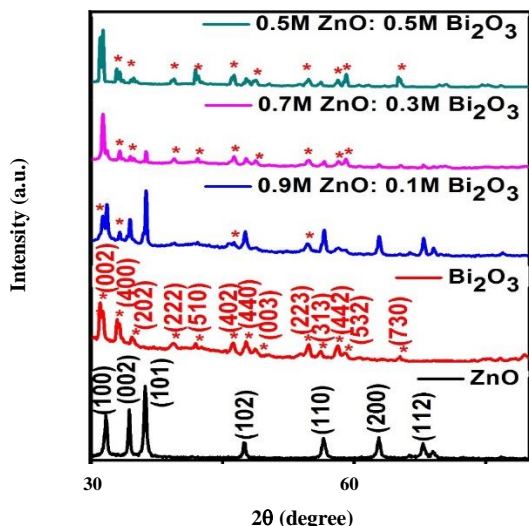


Fig. 1: XRD pattern of ZnO NPs, Bi₂O₃ NPs, and ZnO/Bi₂O₃ NCs.

RESULTS AND DISCUSSION

Structural, optical, and morphological studies

Fig. 1 shows the XRD pattern of ZnO NPs, Bi₂O₃ NPs, and ZnO/Bi₂O₃ NCs. The hexagonal wurtzite structure of ZnO NPs was clear from the diffraction peaks at 2θ values of 32°, 34°, 36°, 47°, 57°, 63° and 68°, indexed with the (100), (002), (101), (102), (110), (103), and (112) planes (JCPDS no. 89-1397) retaining its phase purity [18]. The diffraction peaks of Bi₂O₃ were indexed with (002), (400), (202), (222), (510), (402), (440), (003), (223), (313), (442), (532) and (730) planes (JCPDS No. 74-1374). The average crystallite size was estimated to be 29 nm, 15 nm, 18 nm, 15 nm, and 12 nm for ZnO NPs, Bi₂O₃ NPs, 0.9M ZnO: 0.1M Bi₂O₃, 0.7M ZnO: 0.3M Bi₂O₃, and 0.5M ZnO: 0.5M Bi₂O₃ NCs respectively by using Scherrer's formula. The increase in the peak width of the X-ray peaks corresponds to the reduction in the crystallite size [19]. An increase in Bi concentration is subjected to a continuous increase of the crystallite size. Consequently, a decrease in the particle size results in better photocatalytic activity due to its large surface area.

Fig. 2(a) shows the UV-visible DRS analysis absorbance spectra of as-prepared ZnO NPs, Bi₂O₃ NPs, and ZnO/Bi₂O₃ NCs. ZnO/Bi₂O₃ NCs show absorption both in the UV and visible region [20]. It is obvious that the absorption abilities of the samples were almost the same in the visible region. The energy band gaps (E_g) of ZnO NPs, Bi₂O₃ NPs, and ZnO/Bi₂O₃ NCs were calculated using Tauc's plot. The evaluated bandgap

energy of ZnO NPs, 0.9M ZnO: 0.1M Bi₂O₃, 0.7M ZnO: 0.3M Bi₂O₃ and 0.5M ZnO: 0.5M Bi₂O₃ are 3.14eV, 2eV, 2.35eV and 2.82eV respectively (Fig. 2(b) and (c)) [21]. The formation of electron-hole pairs at the photocatalyst surfaces increases greatly, resulting in the ZnO/Bi₂O₃ NCs exhibiting higher photocatalytic activity. So, the enhanced photocatalytic activity is facilitated by the presence of Bi₂O₃ in ZnO. The bandgap is proportional to the inverse size of nanoparticles, resulting in an increase in the bandgap (E_g) and the carrier concentration of ZnO/Bi₂O₃ NCs [22].

Fig. 3 shows the SEM images of ZnO NPs, Bi₂O₃ NPs, and ZnO/Bi₂O₃ NCs at 5 μ m, 500 μ m, 10 μ m, and 20 μ m magnifications respectively. The as-prepared ZnO and Bi₂O₃ NPs were agglomerated coral reef-like and chunk-like morphology respectively, whereas the ZnO/Bi₂O₃ NCs were square-like morphology. It can be seen that the ZnO and Bi₂O₃ NPs forming composed of nanoparticles having a square shape. The morphological sizes of ZnO/Bi₂O₃ NCs were found ranging between 20 nm - 35 nm. The incorporation of a large amount of Bi₂O₃ in ZnO has resulted in the morphological changes of the ZnO/Bi₂O₃ NCs with cracked surfaces. The transformation of nanoflowers into nanosquares also resulted in the increase in surface area to volume ratio of the ZnO/Bi₂O₃ NCs, and thereby helping in better photocatalytic activity.

Photoluminescence (PL) of ZnO/Bi₂O₃ Nanocomposites

The PL emission is an efficient method to examine the separate efficiency of photoexcited electron-hole pairs and obliging in understanding electron-hole pairs in semiconductor photocatalysts [23]. Fig. 4 shows the PL spectra of the synthesized ZnO NPs, Bi₂O₃ NPs, and ZnO/Bi₂O₃ NCs. The measurement was performed at room temperature. The spectra show strong UV emission peaks with the central wavelength at around 428 nm, 419 nm, and 430 nm for ZnO NPs, Bi₂O₃ NPs, and ZnO/Bi₂O₃ NCs. The PL emission intensity of 0.5M ZnO: 0.5M Bi₂O₃ is significantly smaller than that of other prepared samples, suggesting a lower recombination rate of photogenerated charge carriers in 0.5M ZnO: 0.5M Bi₂O₃, which may explain enhanced photocatalytic performance of 0.5M ZnO: 0.5M Bi₂O₃ compared to the other nanoparticles. The variation in the PL intensity results from the different amounts of strain accumulated in the nanostructures due to their various size and morphology. Because of the more uniform distribution, the NCs show high intense excitonic

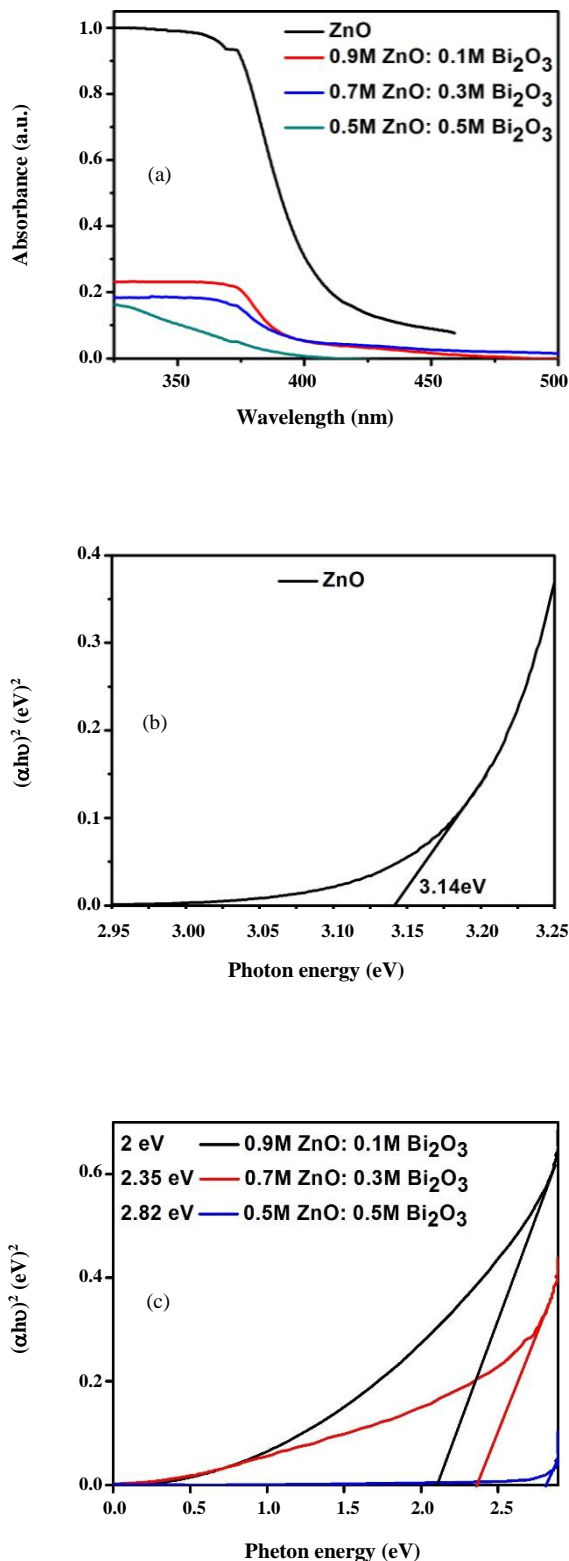


Fig. 2: (a) Absorption spectra of ZnO NPs, Bi₂O₃ NPs, and ZnO/Bi₂O₃ NCs (b) and (c) Tauc's plot of $(ah\nu)^2$ versus Photon energy.

peak, making clear that the luminescence properties of ZnO can be controlled by changing its morphology. The Bi₂O₃ doped ZnO is slightly red-shifted from that of pure ZnO and Bi₂O₃ nanoflowers. This shows that Bi₂O₃ affects ZnO PL spectrum [24]. The photoluminescence spectrum of the nanoparticles is attributed to the radiative recombination process of self-trapped excitations. The intensity for Bi₂O₃ doped ZnO indicates that radiative recombination was lowered, leading to weak recombination of the electron-hole pairs and high photo efficiency. Hence, the results suggest that the 0.5M ZnO: 0.5M Bi₂O₃ NCs had the highest photo efficiency examined in this work and could be used as an effective photocatalyst.

Photocatalytic Degradation of acid and basic dyes

The photocatalytic activities of ZnO NPs, Bi₂O₃ NPs, and ZnO/Bi₂O₃ NCs were evaluated by the degradation of basic dyes Methyl Blue (MB), Malachite Green (MG), and Rhodamine 6G (R6G) under visible light irradiations for 120 mins respectively. The rate of decomposition of basic dyes, using ZnO NPs, Bi₂O₃ NPs, and ZnO/Bi₂O₃ NCs under visible light irradiation (Fig. 5), proves a good linear correlation of rate constants. The rate constants were estimated quantitatively for MB as $3 \times 10^{-3}/\text{min}$, $8 \times 10^{-3}/\text{min}$, $5 \times 10^{-3}/\text{min}$, $8 \times 10^{-3}/\text{min}$, $8.5 \times 10^{-3}/\text{min}$, and $9 \times 10^{-3}/\text{min}$, for MG as $8 \times 10^{-3}/\text{min}$, $5 \times 10^{-3}/\text{min}$, $2 \times 10^{-3}/\text{min}$, $3 \times 10^{-3}/\text{min}$, $6 \times 10^{-3}/\text{min}$ and $7 \times 10^{-3}/\text{min}$ and R6G as $2.5 \times 10^{-3}/\text{min}$, $5 \times 10^{-3}/\text{min}$, $1 \times 10^{-3}/\text{min}$, $1.3 \times 10^{-3}/\text{min}$, $2 \times 10^{-3}/\text{min}$ and $9 \times 10^{-3}/\text{min}$ under visible light irradiation, by the pseudo-first-order reaction [25] and plotted as $\ln(C_t/C_0)$ versus time (minutes). E_g widening [26], increased visible light absorption, inhibition of the electron-hole recombination and increased number of oxygen vacancies or defects are responsible for the augmented photocatalytic ability of 0.5M ZnO: 0.5M Bi₂O₃ NCs in dye. The photogenerated carriers in smaller particles are also likely to transfer more quickly to the samples surface without recombination [27]. Among the three basic dyes, MB and MG degraded effectively in 90mins with 93% efficiency, whereas R6G degraded at 120mins with an efficiency of 89% when mixed with 0.5M ZnO: 0.5M Bi₂O₃ NCs. This efficient activity can be ascribed to its stronger absorption ability for visible light and better charge carrier separation.

The electrons in the conduction band of ZnO/Bi₂O₃ NCs reduce molecular oxygen and produce the superoxide

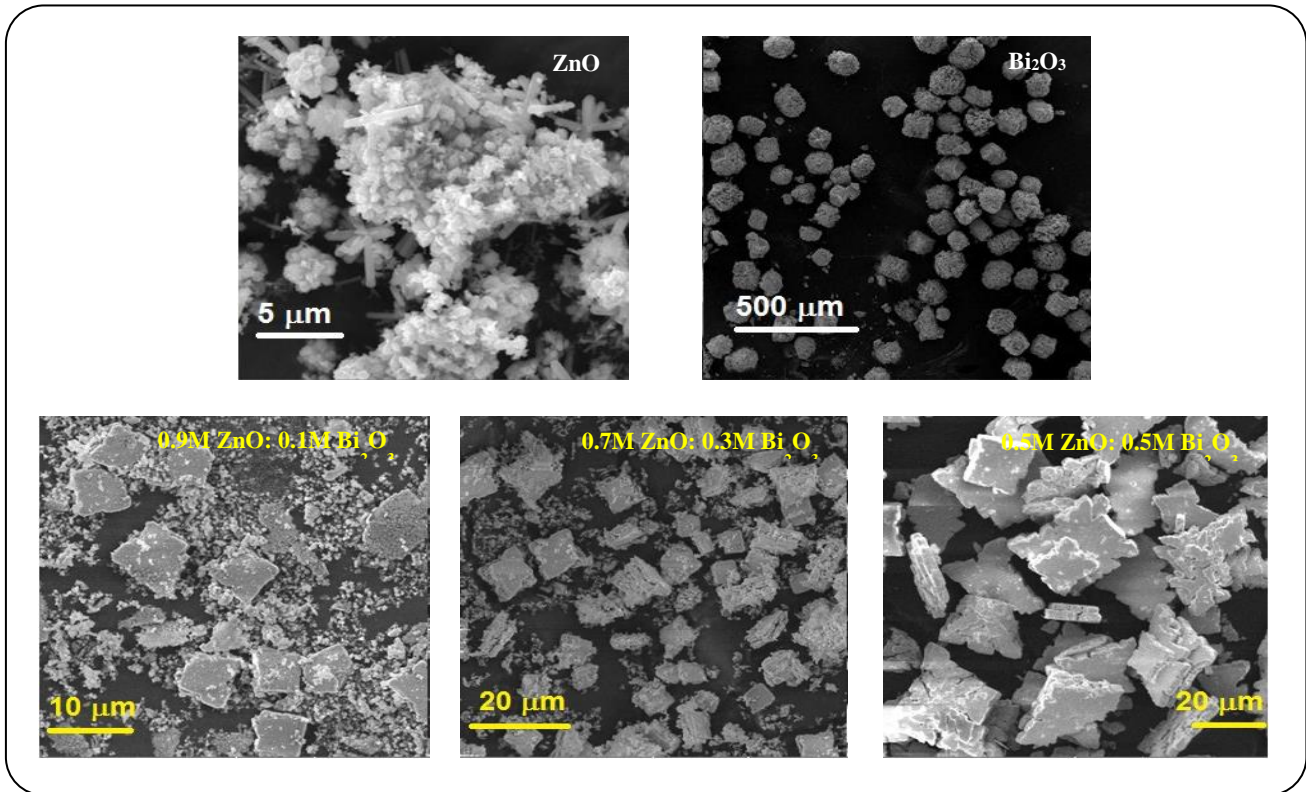


Fig. 3 SEM images of ZnO NPs, Bi₂O₃ NPs, and ZnO/Bi₂O₃ NCs

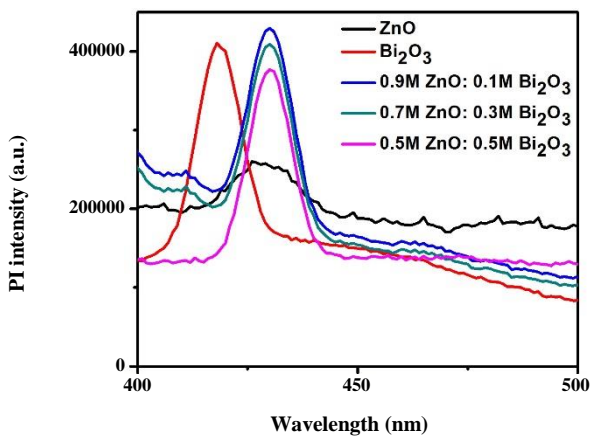
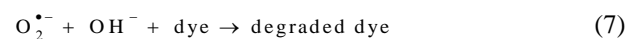


Fig. 4: Photoluminescence spectra of ZnO NPs, Bi₂O₃ NPs, and ZnO/Bi₂O₃ NCs.

anion radical when irradiated by UV and visible light. The Mechanism of photodegradation of dyes under visible light is as shown in Fig. 5(d). The formation of free radicals in photocatalytic reaction mechanism is as illustrated below:



The hydroxide (OH[•]) radicals were able to oxidize the pollutant molecules into CO₂ and H₂O owing to their high oxidative capacity. OH[•] radicals are powerful oxidizing agents, capable of attacking organic pollutants by the formation of intermediates that produce photocatalytic products. The trapping of the photogenerated electron on Bi₂O₃ defective sites and holes on ZnO NPs, allows wider charge separation and light recombination, thereby leading to photocatalytic enhancement [28]. In ZnO crystallinity, the oxygen vacancy defects act as the recombination centers to capture photoelectrons [29]. 0.5M ZnO: 0.5M Bi₂O₃ is more easily activated by the light irradiation of

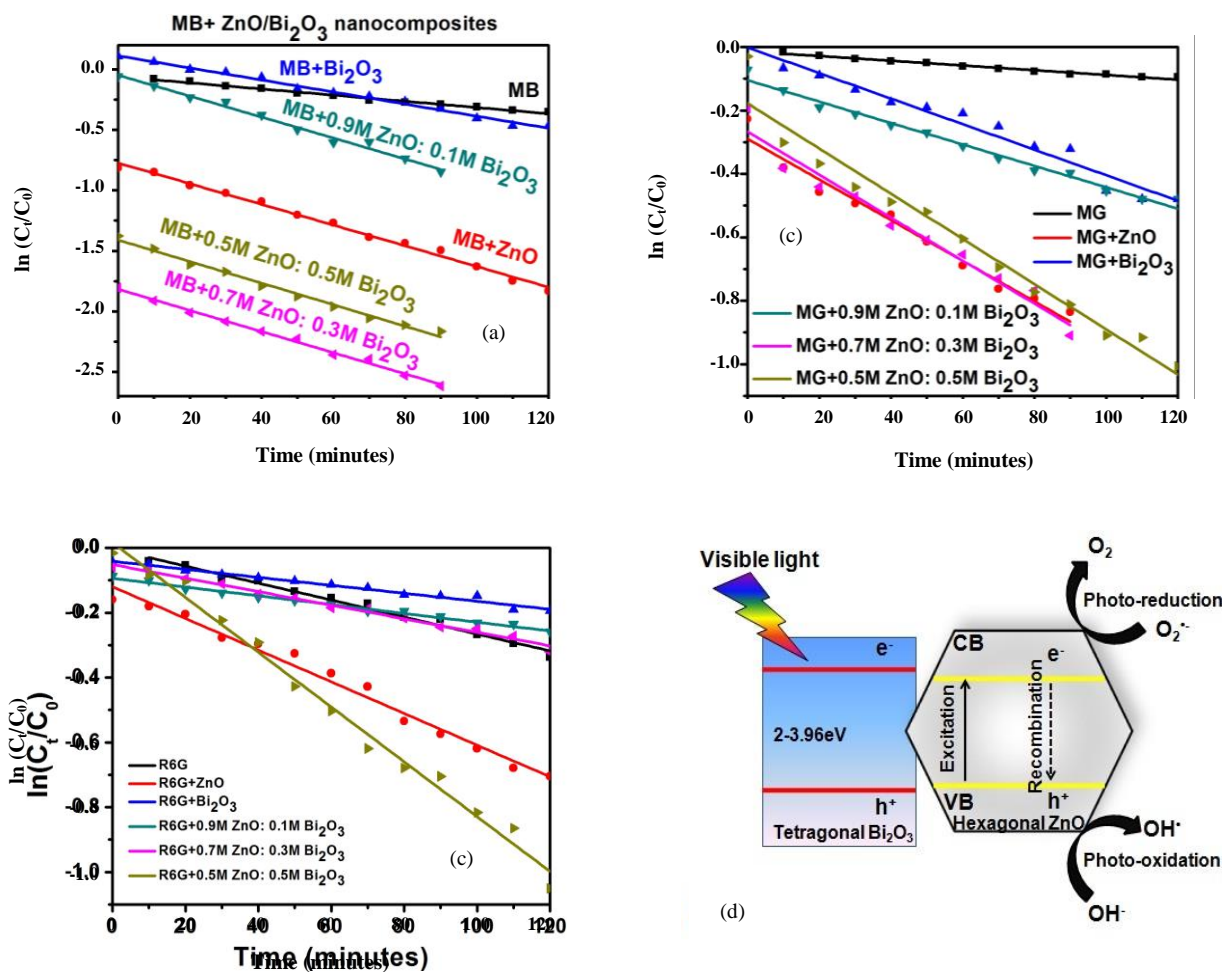


Fig. 5: Rate of decomposition of (a) MB (b) MG and (c) R6G using ZnO NPs, Bi₂O₃ NPs, and ZnO/Bi₂O₃ NCs under visible light irradiation versus irradiation time and (d) Mechanism of photodegradation of dyes

long-wavelength to generate conduction band electrons and valence band holes due to its smaller energy gaps [30]. The decomposition of dyes is facilitated by electrons and holes thereby leading to the formation of highly reactive radicals, namely hydroxyl radicals (OH[•]) and superoxide (O₂⁻). Hence ZnO/Bi₂O₃ NCs prove to be a suitable candidate in degrading and decolorizing wastewater in dyeing industries.

Antibacterial activity

The antibacterial activity of the prepared ZnO NPs, Bi₂O₃ NPs, and ZnO/Bi₂O₃ NCs was measured against the gram-positive *S. aureus* (Fig. 6(a)) and gram-negative *E. coli* (Fig. 6(b)) by disc diffusion method. Three different concentrations of each sample namely 25 μ L, 50 μ L, and 75 μ L were taken in the disc of 5mm in diameter.

The plates were incubated for 24 h at 37 °C. Chloramphenicol 10 μ g was used as the control against the bacterial strains. Table 1 shows the zone of inhibition (mm) of ZnO NPs, Bi₂O₃ NPs, and ZnO/Bi₂O₃ NCs at 75 μ L concentration. It is observed that 0.5M ZnO: 0.5M Bi₂O₃ NCs showed significant antibacterial activities against *S. aureus* (6mm) and *E. coli* (5mm) (Fig. 6(c)). As the surface area of ZnO/Bi₂O₃ NCs increases, so also does the OH[•] concentration on this surface resulting in the bactericidal activity of pathogens [31]. Due to the production of OH[•] in the samples penetrates the cell membrane and damages the DNA and cell protein and leads to cell death [32]. The 0.5M ZnO: 0.5M Bi₂O₃ NCs shows higher antibacterial activity against *S. aureus* and *E. coli* when compared to the other NCs. The reported antibacterial activity has shown if Fig. 6(d) is due to

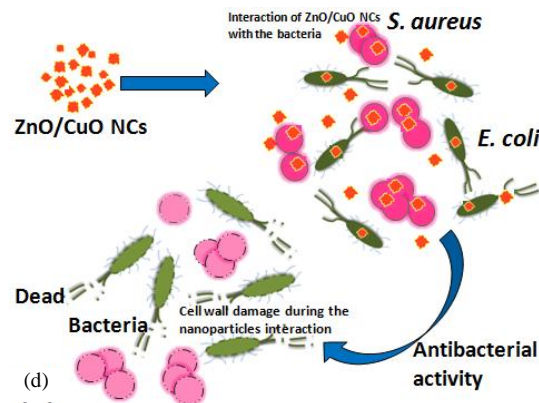
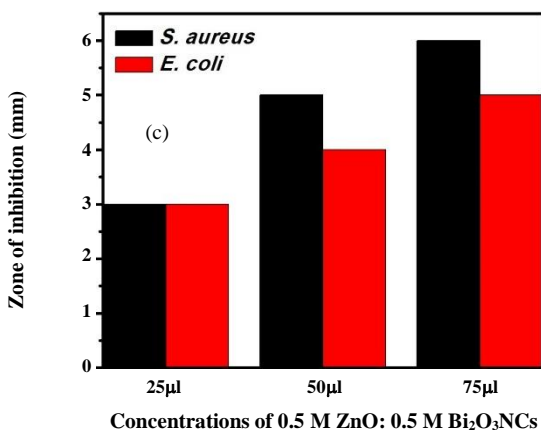
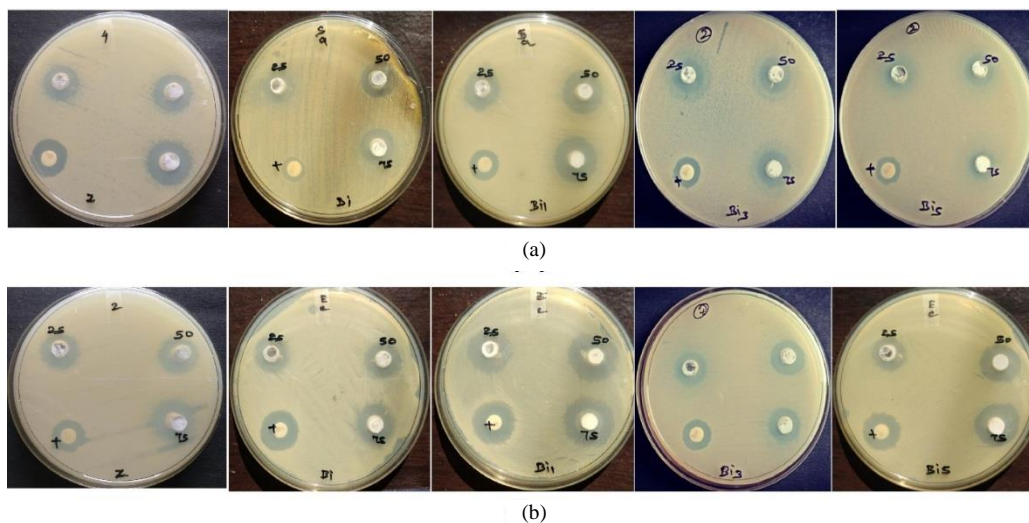


Fig. 6: Antibacterial activity of ZnONPs, Bi₂O₃ NPs and ZnO/ Bi₂O₃ NCs against (a) *S. aureus* and (b) *E. coli* (c) Graphical representation of 0.5M ZnO: 0.5M Bi₂O₃ NCs against *E. coli* and *S. aureus* and (d) Mechanism of antibacterial activity by ZnO/CuO NCs

the interaction of ZnO/CuO NCs with the negatively charged bacterial cell surface and resulting in cell damage [33]. Moreover, these NCs with better photocatalytic activity have larger specific surface areas and smaller crystal size increases, oxygen vacancies, and the OH⁻ concentration on their surface which causes an increase in the O²⁻ concentration and destruction of the cell wall of the pathogens [34]. Superoxide anions O²⁻ react with peptide linkages in the cell walls of bacteria or spores and destroy them [35]. The higher deactivation efficiency in the case of gram-negative bacteria as compared to the gram-positive pathogen was reported earlier [36]. Thus the results obtained in this study illustrate the possibilities of using synthesized NCs as photocatalysts and antibacterial agents.

CONCLUSIONS

New insights for the preparation of ZnO/Bi₂O₃ NCs hydrothermally with selective weight percentage were proposed. ZnO/Bi₂O₃ NCs were characterized by using XRD, UV-visible, and SEM. Variations in Bi concentration have an influence on the particle size. XRD reveals that the synthesized ZnO/Bi₂O₃ NCs are not a single phase but are of a composite nature with a hexagonal wurtzite structure. SEM disclosed the square-like structure of the ZnO/Bi₂O₃ NCs. These NCs showed exceptionally high visible-light photocatalytic performance for basic dyes compared with that of the individual ZnO and Bi₂O₃ NPs. The improved photocatalytic activity can be attributed to the contributions of the energy level position, separation

Table 1: Zone of inhibition (mm) of ZnO NPs, Bi₂O₃ NPs and ZnO/Bi₂O₃ NCs at 75µL concentration.

Samples	S. aureus (10 µg/ mL)	Standard Chloramphenicol (10 µL/ mL)	E. coli (10 µg/ mL)	Standard Chloramphenicol (10 µL/ mL)
ZnO NPs	5	5	5	6
Bi ₂ O ₃ NPs	5	6	5	6
0.9M ZnO: 0.1M Bi ₂ O ₃	4	6	4	6
0.7M ZnO: 0.3M Bi ₂ O ₃	5	6	4	6
0.5M ZnO: 0.5M Bi ₂ O ₃	6	6	5	6

of photogenerated electron-hole pairs, enlarged surface areas, and remarkably enhanced light absorption. Better antibacterial activity is supposed to be caused by the electrostatic forces between the ZnO/Bi₂O₃ NCs. Thus the study not only provides insight for the preparation of NCs photocatalysts but also demonstrates the feasibility of utilizing the cheap and abundant ZnO and Bi to replace the precious noble metals for enhancing photocatalysis efficiency in degrading and decolorizing the basic dyes used in textile industries and thereby inhibiting the pathogenic bacteria efficiently.

Acknowledgment

This work was supported by the University Grants Commission-Rajiv Gandhi National Fellowship [F1-17.1/2016-17/RGNF-2015-17-SC-TAM-23657/(SA-III/Website)], New Delhi.

Received : Dec. 15, 2019 ; Accepted : May 25, 2020

REFERENCES

- [1] Lai C., Wang M.M., Zeng G.M., Liu Y.G., Huang D.L., Zhang C., Wang R.Z., Xu P., Cheng M., Huang C., [Synthesis of Surface Molecular Imprinted TiO₂/Graphene Photocatalyst and its Highly Efficient Photocatalytic Degradation of Target Pollutant Under Visible Light Irradiation](#), *Appl. Surf. Sci.*, **390**: 368-376 (2016).
- [2] Saratale R.G., Saratale G.D., Chang J.S., Govindwar S.P., [Bacterial Decolorization and Degradation of Azo Dyes: A Review](#), *J. Taiwan Inst. Chem. Eng.* **42**: 138-157 (2011).
- [3] Sobczynski A., Dobosz A., [Water Purification by Photocatalysis on Semiconductors](#), *Pol. J. Environ. Stud.* **10(4)**: 195–205 (2001).
- [4] Fan H., Jiang T., Wang L., Wang D., Li H., Wang P., [Effect of BiVO₄ Crystalline Phases on the Photoinduced Carriers Behavior and Photocatalytic Activity](#), *J. Phys Chem.*, **116(3)**: 2425-2430 (2012)
- [5] Agarwal H., Kumar S.V., Rajeshkumar S., [A Review on Green Synthesis of Zinc Oxide Nanoparticles – An Eco-Friendly Approach](#), *Resour. Technol.*, **3(4)**: 406-413 (2017)
- [6] Kim H.G., Hwang D.W., Lee J.S., [An Undoped, Single-Phase Oxide Photocatalyst Working under Visible Light](#), *J. Am. Chem. Soc.* **126**: 8912-8913 (2004)
- [7] Zhou L., Wang W.Z., Xu H.L., Sun S.M., Shang M., [Bi₂O₃ Hierarchical Nanostructures: Controllable Synthesis, Growth Mechanism, and Their Application in Photocatalysis](#), *Chem. A Eur. J.* **15**: 1776 – 1782 (2009)
- [8] Fruth V., Popa M., Berger D., Ramer R., Gartner M., Ciulei A., Zaharescu M., [Deposition and Characterization of Bismuth Oxide Thin Films](#), *J. Eur. Ceram. Soc.*, **25**: 2171-2174 (2005)
- [9] Vijayaraghavan G., Shanthakumar S., [Effective Removal of Acid Black 1 Dye in Textile Effluent Using Alginate from Brown Algae as a Coagulant](#), *Iran. J. Chem. Chem. Eng(IJCCE)*, **37(4)**:145-151 (2018)
- [10] Lade H.S., Waghmode T.R., Kadam A.A., Govindwar S.P., [Enhanced Biodegradation and Detoxification of Disperse Azo Dye Rubine GFL and Textile Industry Effluent by Defined Fungal-Bacterial Consortium](#), *Int. Biodeterior. Biodegrad.*, **72**: 94-107 (2012).
- [11] Gao S., Jia X., Yang S., Li Z., Jiang K., [Hierarchical Ag/ZnO Micro/Nanostructure: Green Synthesis and Enhanced Photocatalytic Performance](#), *J. Solid State Chem.* **184**: 764-769 (2011).

- [12] Saravanan R., Karthikeya S., Gupta V.K., Sekaran G., Narayanan V., Stephen A., [Enhanced Photocatalytic Activity of ZnO/CuO Nanocomposite for the Degradation of Textile Dye on Visible Light Illumination](#), *Mater. Sci. Eng. C.*, **33**: 91-98 (2013).
- [13] Chandraboss V.L., Natanapatham L., Karthikeyan B., Kamalakkannan J., Prabha S., Senthilvelan S., [Effect of Bismuth Doping on the ZnO Nanocomposite Material and Study of its Photocatalytic Activity under UV-light](#), *Mater. Res. Bull.*, **40**: 3707-3712 (2013).
- [14] Tongqin C., Zijiong L., Gaoqian Y., Yong J., Hongjun Y., [Enhanced Photocatalytic Activity of ZnO/CuO Nanocomposites Synthesized by Hydrothermal Method](#), *Nano-Micro Lett.* **5**(3): 163-168 (2013).
- [15] Weidong H., Wei Q., Xiaohong W., Xianbo D., Long C., Zhaohua J., [The Photocatalytic Properties of Bismuth Oxide Films Prepared Through the Sol-Gel Method](#), *Thin Solid Films* **515**: 5362–5365 (2007).
- [16] ComLekcioglu N., Aygan A., Kutlu M., [Antimicrobial Activities of Some Natural Dyes and Dyed Wool Yarn](#), *Iran. J. Chem. Chem. Eng. (IJCCE)*, **36**(4): 137-144 (2017).
- [17] Dar M.A., Kim Y.S., Kim W.B., Sohn J.M., Shin H.S., [Structural and Magnetic Properties of CuO Nanoneedles Synthesized by Hydrothermal Method](#), *Appl Surf Sci.* **254**: 7477–7481 (2008).
- [18] Ali F., Sajjad B., [Comparison Studies of Adsorption Properties of MgO Nanoparticles and ZnO–MgO Nanocomposites for Linezolid Antibiotic Removal From Aqueous Solution Using Response Surface Methodology](#), *Process Saf. Environ. Prot.*, **94**: 37-43 (2015).
- [19] Irmawati R., Noorfarizan Nasriah M.N., Taufiq-Yap Y.H., Abdul Hamid S.B., [Characterization of Bismuth Oxide Catalysts Prepared from Bismuth Trinitrate Pentahydrate: Influence of Bismuth Concentration](#), *Catalysis Today.*, **93–95**: 701–709 (2004).
- [20] Subramanian B., Meenakshisundram S., [Facile Fabrication of Heterostructured Bi₂O₃–ZnO Photocatalyst and Its Enhanced Photocatalytic Activity](#), *J. Phys. Chem. C.* **116**: 26306–26312 (2012).
- [21] Movahedi M., Hosseinian A., Nasrin N., Rahimi M, Salavati H., [Synthesis of ZnO/Bi₂O₃ and SnO₂/Bi₂O₃/Bi₂O₄ Mixed Oxides and Their Photocatalytic Activity](#), *Iran. Chem. Commun.* **3**: 374-387 (2015).
- [22] Li H., Zhang Y., Pan X., Zhang H., Wang T., Xie E., [Effects of In and Mg Doping on Properties of ZnO Nanoparticles by Flame Spray Synthesis](#), *J. Nanopart. Res.* **11**: 917-921(2009).
- [23] Dong F., Zhao Z.W., Sun Y.J., Zhang Y.X., Yan S., Wu Z.B., [An Advanced Semimetal–Organic Bi Spheres–g-C₃N₄ Nanohybrid with SPR-Enhanced Visible-Light Photocatalytic Performance for NO Purification](#), *Environ. Sci. Technol.* **49**: 12432–12440 (2015).
- [24] Congkang Xu, Keehan Rho, Junghwan Chun, Dong Eon Kim, [Fabrication and Photoluminescence of ZnO Hierarchical Nanostructures Containing Bi₂O₃](#), *Nanotechnol* **17**: 60-64 (2006).
- [25] Raj R.B., Umadevi M., Parvathi V.P., Parimaladevi R., [Effect of Potassium on Structural, Photocatalytic and Antibacterial Activities of ZnO Nanoparticles](#), [Effect of Potassium on Structural, Photocatalytic and Antibacterial Activities of ZnO Nanoparticles](#), *Adv. Nat. Sci. Nanosci. Nanotechnol* **7**: 45008 (2016).
- [26] Shuwang D., Yangyanghi, Hao Z., Tingzhi L., Kai W., Zaiquan L., [A Facile Salicylic Acid Assisted Hydrothermal Synthesis of Different Flower-Like ZnO Hierarchical Architectures With Optical and Concentration-Dependent Photocatalytic Properties](#), *Mater. Charact* **114**: 185-196 (2016).
- [27] Hagfeldt A., Graetzel M., [Light-Induced Redox Reactions in Nanocrystalline Systems](#), *Chem. Rev.* **95**: 49-68 (1995).
- [28] Bandara J., Haghdar C.C., Jayasekera W.G., [TiO₂/MgO Composite Photocatalyst: the Role of MgO in Photoinduced Charge Carrier Separation](#), *Appl. Catal. B Environ.* **50**: 83-88 (2004).
- [29] Zhu Z., Yang D., Liu H., [Microwave-Assisted Hydrothermal Synthesis of ZnO Rod-Assembled Microspheres and Their Photocatalytic Performances](#), *Adv. Powder Technol.* **22**: 493-497 (2011).
- [30] He Weidong, Qin Wei, Wu Xiaohong, Ding Xianbo, Chen Long, Jiang Zhaohua, [The Photocatalytic Properties of Bismuth Oxide Films Prepared through the Sol-Gel Method](#), *Thin Solid Films.* **515**(13): 5362-5365 (2007).
- [31] Venkateswara Reddy P., Venkatramana Reddy S., Sankara Reddy B., [Synthesis and Properties of \(Fe, Al\) Co-Doped SnO₂ Nanoparticles](#), *Mater. Today Proc.* **3**: 1752-1761 (2016).

- [32] Chandran D., Nair L.S., Balachandran S., Rajendra Babu K., Deepa M., [Structural, Optical, Photocatalytic and Antimicrobial Activities of Cobalt-Doped Tin Oxide Nanoparticles](#), *J. Sol-Gel Sci. Technol.* **76(3)**: 582-591 (2015).
- [33] Revathi T., Thambidurai S., [Immobilization of ZnO on Chitosan-Neem Seed Composite for Enhanced Thermal and Antibacterial Activity](#), *Adv. Powder Technol.* **29(6)**: 1445-1454 (2018).
- [34] Gordon T., Perlstein B., Houbara O., Felner I., Banin E., Margel S., [Synthesis and Characterization of Zinc/Iron Oxide Composite Nanoparticles and Their Antibacterial Properties](#), *Colloids Surf A: Physicochem Eng Asp.* **374(1)**: 1-8 (2011).
- [35] Chunxu D., DeLong S., John C., Orville Lee M., Gaohong H., Yulin D., [Antibacterial Study of Mg\(OH\)₂ Nanoplatelets](#), *Mater. Res. Bull.* **46**: 576-582 (2011).
- [36] Pal A., Pehkonen S.O., Yu L.E., Ray M.B., [Photocatalytic Inactivation of Gram-Positive and Gram-Negative Bacteria Using Fluorescent Light](#), *J. Photochem. Photobiol. A Chem.*, **186**: 335-341 (2007).